Demagnetizing Field in Nonellipsoidal Bodies

R. I. Joseph and E. Schlömann

Citation: Journal of Applied Physics **36**, 1579 (1965); doi: 10.1063/1.1703091
View online: http://dx.doi.org/10.1063/1.1703091
View Table of Contents: http://scitation.aip.org/content/aip/journal/jap/36/5?ver=pdfcov
Published by the AIP Publishing

F. Comparison with InSb Diodes

Similar studies have been made with both spontaneously emitting and laser diodes of InSb.[8] There, the magnetic shift and the photon energy of the emission observed can be accounted for by band-to-band transitions. Although the magnetic shift proceeds in a manner similar to that of InAs diodes and there is a very pronounced spin splitting, the threshold in InSb lasers is greatly reduced by magnetic fields *parallel* to the diode current. This has been explained in terms of an increased transition probability resulting from a condensation of energy states. The absence of this effect in InAs lasers may be associated with the fact that the transition probability is already close to unity without the relatively large fields required for appreciable condensation of states. Such high quantum efficiencies would be expected from the external quantum efficiencies of up to 25% which have been reported[22] for InAs diode lasers.

ACKNOWLEDGMENTS

The authors thank W. D. Fife and C. R. Grant for technical assistance and Mary L. Barney and L. J. Belanger for fabrication of the InAs diodes.

JOURNAL OF APPLIED PHYSICS VOLUME 36, NUMBER 5 MAY 1965

Demagnetizing Field in Nonellipsoidal Bodies*

R. I. Joseph and E. Schlömann
Raytheon Research Division, Waltham, Massachusetts
(Received 6 November 1964)

A general method for calculating the (nonuniform) demagnetizing field in ferromagnetic bodies of arbitrary shape is described. The theory is based upon the assumption that the magnitude of the magnetization vector is constant throughout the sample and that its direction coincides with the direction of the local magnetic field at any point within the sample. The total magnetic field is expressed as a series of ascending powers in M/H_0, where M is the saturation magnetization and H_0 the applied magnetic field. The first term of this series expansion (first-order theory) gives the demagnetizing field for very large applied fields, i.e., for a uniformly magnetized sample. The higher-order corrections (we consider in detail only the first correction term; second-order theory) take account of the fact that the sample is not in general uniformly magnetized. The general theory has been applied to rectangular slabs and circular cylinders. The first-order demagnetizing field has been calculated for rectangular slabs and circular cylinders of arbitrary dimensions. Our discussion of the second-order theory is restricted to the semi-infinite slab and the semi-infinite circular cylinder. For the semi-infinite slab the variation of the second-order demagnetizing field along the central symmetry axis and across the endface have been calculated. In cases of practical interest (spin-wave propagation experiments in YIG at 3 Gc/sec and applied magnetic field of about 1400 Oe), the second-order correction to the demagnetizing factor is approximately 20% of the first-order contribution.

I. INTRODUCTION

It is well known that the surface divergence of the magnetization vector gives rise to a magnetic field, usually termed the "demagnetizing field."[1] In ellipsoidal bodies which are uniformly magnetized the demagnetizing field is in turn also uniform. In nonellipsoidal bodies, however, the demagnetizing field is in general nonuniform.[2] Experimental data taken on nonellipsoidal samples are, therefore, usually extremely difficult to interpret. For this reason most experiments on ferro- or ferrimagnetic materials are performed on samples of ellipsoidal shape. Quite frequently, however, other considerations make it advantageous to use samples that have a nonellipsoidal shape; for instance, rectangular prisms, or cylinders with flat endfaces. In recent experiments on spin-wave propagation,[3] for instance, the nonuniformity of the demagnetizing field largely determines the excitation efficiency and the velocity of propagation in the sample.[4] In cases like this, it is important to know the demagnetizing field as a function of position throughout the sample. The work reported in this paper is directed towards this aim.[5]

The demagnetizing field, as its name suggests, tends to demagnetize the sample. In the experiments considered

* Supported in part by the U. S. Army Electronics Laboratory under Contract No. DA36-039-AMC-00064(E).

[1] W. F. Brown, Jr., *Magnetostatic Principles in Ferromagnetism* (North-Holland Publishing Company, Amsterdam, 1962).

[2] The infinite cylinder and the infinite sheet should be regarded as limiting cases of the class of ellipsoidal bodies. The toroid is substantially equivalent with an infinite cylinder.

[3] J. R. Eshbach, Phys. Rev. Letters 8, 357 (1962); J. Appl. Phys. 34, 1298 (1963).

[4] E. Schlömann in *Advances in Quantum Electronics*, edited by J. R. Singer (Columbia University Press, New York, 1961), p. 437; E. Schlömann, J. Appl. Phys. 35, 159 (1964); E. Schlömann and R. I. Joseph, J. Appl. Phys. 35, 167 (1964); E. Schlömann and R. I. Joseph, J. Appl. Phys. 35, 2382 (1964); E. Schlömann and R. I. Joseph, J. Appl. Phys. 36, 875 (1965).

[5] Recent experimental results, which are in agreement with the calculations described in this paper have been presented by T. Kohane, E. Schlömann, and R. I. Joseph, 1964 Conference on Magnetism and Magnetic Materials, paper O2 and J. Appl. Phys. Suppl. 36, 1267 (1965).

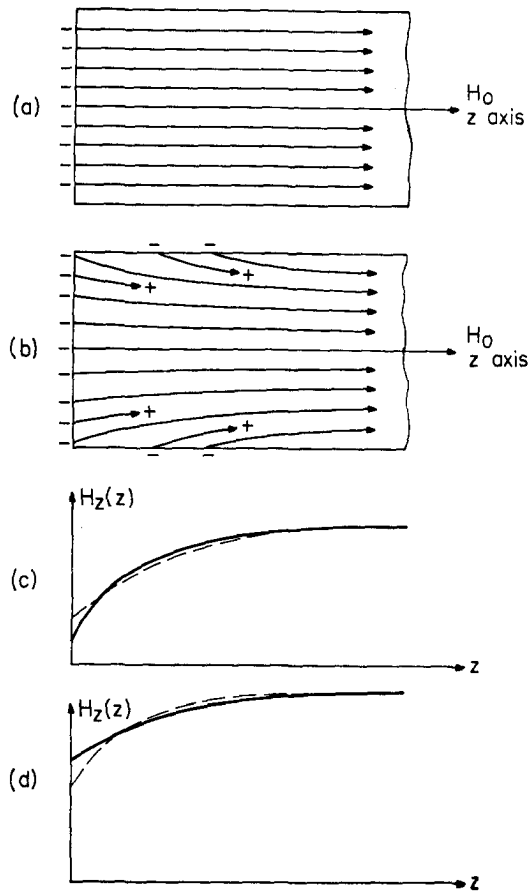

FIG. 1. (a) Cross section of long rectangular prism or cylinder showing the field lines for uniform magnetization (very large applied fields); (b) Same geometry as (a), but now showing the field lines for the actual distribution of magnetization at applied fields comparable to $4\pi M$; (c) z component of net magnetic field along the center axis of the sample shown in (a) and (b) (broken line: uniform magnetization, full line: actual magnetization); (d) z component of net magnetic field along the sideface [otherwise, same as (c)].

above, this tendency is counteracted by an externally applied magnetic field. If the applied magnetic field is sufficiently large the sample will become substantially uniformly magnetized even though the demagnetizing field is nonuniform. We, therefore, express the total magnetic field as a series of ascending powers in M/H_0, where M is the saturation magnetization and H_0 the applied magnetic field. The general theory of the demagnetizing field is described in Sec. II. The first term of the series expansion in M/H_0 gives the demagnetizing field at very large applied fields, i.e., for a uniformly magnetized sample. This "first approximation" is evaluated for rectangular prisms in Sec. IIIA and for longitudinally magnetized circular cylinders in Sec. IVA. For rectangular prisms the result can be expressed in terms of elementary functions, for circular cylinders as an integral over Bessel functions or equivalently in terms of elliptic integrals. The "second approximation" of the demagnetizing field is much more difficult to evaluate than the first approximation. For this reason we confine our attention to the semi-infinite slab (discussed in Sec. IIIB) and the semi-infinite circular cylinder (discussed in Sec. IVB). The results are discussed in Sec. V.

II. GENERAL THEORY

Let $\boldsymbol{\alpha}(\mathbf{r})$ be a unit vector in the direction of the magnetization at point $\mathbf{r}$. Thus the magnetization $\mathbf{M}(\mathbf{r})$ at this point is given by

$$\mathbf{M}(\mathbf{r})=M\boldsymbol{\alpha}(\mathbf{r}). \tag{1}$$

Here M is the saturation magnetization which we assume to be constant. We further assume that the direction of magnetization at any point in the sample coincides with the direction of the total magnetic field $\mathbf{H}(\mathbf{r})$ at this point. Thus

$$\boldsymbol{\alpha}(\mathbf{r})=\mathbf{H}(\mathbf{r})/|\mathbf{H}(\mathbf{r})|. \tag{2}$$

This assumption becomes invalid because of exchange effects when the sample is very small (less than approximately $1\,\mu$). It also disregards all effects related to magnetic hysteresis. As long as the applied field is appreciably larger than the coercive force and as long as the samples are reasonably large, however, Eq. (2) should represent a very good approximation.

The total field occurring in Eq. (2) is the sum of the applied field $\mathbf{H}_0$ and the demagnetizing field. The latter can be represented as M times the gradient of a potential ψ. Thus

$$\mathbf{H}(\mathbf{r})=\mathbf{H}_0+M\nabla\psi(\mathbf{r}). \tag{3}$$

It should be noticed that the potential ψ, according to this definition, has the dimension of a length.

Because $\mathbf{B}=\mathbf{H}+4\pi\mathbf{M}$ is divergence-free, one obtains

$$\nabla\cdot\mathbf{H}=-4\pi M\nabla\cdot\boldsymbol{\alpha} \tag{4}$$

and hence

$$\nabla^2\psi=-4\pi\nabla\cdot\boldsymbol{\alpha}. \tag{5}$$

Thus the potential ψ can be expressed as a volume integral over $\boldsymbol{\alpha}(\mathbf{r})$.

$$\psi(\mathbf{r})=\int\frac{\boldsymbol{\alpha}(\mathbf{r}')\cdot(\mathbf{r}'-\mathbf{r})}{|\mathbf{r}'-\mathbf{r}|^3}d^3\mathbf{r}'. \tag{6}$$

This follows from the better known formula in which ψ is expressed as the sum of a volume integral and a surface integral over $\nabla\cdot\boldsymbol{\alpha}$, and can also be verified directly.

Insertion of Eq. (3) into Eq. (6) leads to an integral equation for the potential. We construct a solution of this equation as a power series in

$$\epsilon=M/|\mathbf{H}_0|. \tag{7}$$

Thus

$$\psi=\psi_1+\epsilon\psi_2+\epsilon^2\psi_3+\cdots. \tag{8}$$

If we take the direction of $\mathbf{H}_0$ as the z axis of our coordinate system ($|\mathbf{H}_0|\equiv H_0$), it follows from Eqs. (2), (3),

and (8) that

$$\alpha_z = 1 - \tfrac{1}{2}\epsilon^2[(\partial\psi_1/\partial x)^2 + (\partial\psi_1/\partial y)^2] + 0(\epsilon^3)$$
$$\alpha_x = \epsilon(\partial\psi_1/\partial x) + \epsilon^2[(\partial\psi_2/\partial x) - (\partial\psi_1/\partial x)(\partial\psi_1/\partial z)] + 0(\epsilon^3). \quad (9)$$

The expression for α_y is analogous to that for α_x. Combining Eqs. (6) and (9) we find as the first, second, and third approximation

$$\psi_1(\mathbf{r}) = \int \frac{z'-z}{|\mathbf{r}'-\mathbf{r}|^3} d^3\mathbf{r}' \quad (10)$$

$$\psi_2(\mathbf{r}) = \int \frac{(\partial\psi_1/\partial x')(x'-x) + (\partial\psi_1/\partial y')(y'-y)}{|\mathbf{r}'-\mathbf{r}|^3} d^3\mathbf{r}' \quad (11)$$

$$\psi_3(\mathbf{r}) = \int \{[(\partial\psi_2/\partial x') - (\partial\psi_1/\partial x')(\partial\psi_1/\partial z')](x'-x) + [(\partial\psi_2/\partial y') - (\partial\psi_1/\partial y')(\partial\psi_1/\partial z')](y'-y) - \tfrac{1}{2}[(\partial\psi_1/\partial x')^2 + (\partial\psi_1/\partial y')^2](z'-z)\} \times |\mathbf{r}'-\mathbf{r}|^{-3} d^3\mathbf{r}'. \quad (12)$$

In the following we consider only ψ_1 and ψ_2.

Before attempting to evaluate the integrals of Eqs. (10) and (11) for any particular sample shape, it is worthwhile to derive some qualitative relationships. Consider, for instance, a long rectangular prism or a long circular cylinder with flat, perpendicular endfaces. Figures 1(a) and 1(b) show the cross section of such a sample. If the sample is sufficiently long the demagnetizing field near each endface is substantially independent of the divergence of the magnetization at the other endface, so that the sample may be considered as infinitely long. If the applied field is very large the sample becomes substantially uniformly magnetized. Figures 1(a) and 1(b) also show the field lines of the magnetization vector. Figure 1(a) corresponds to uniform magnetization. Since the demagnetizing field associated with this distribution of magnetization is nonuniform, the magnetization can also not be uniform. Figure 1(b) shows, in a qualitative way, the field lines of the resultant distribution of magnetization. It should be noticed that in addition to a surface divergence at the endface ($z=0$), a surface divergence now also occurs at the sidefaces and also a volume divergence. The sign of the "effective magnetic charge" (negative divergence of magnetization) is indicated by plus and minus signs in Figs. 1(a) and 1(b). The surface divergence at the endface is reduced by comparison with the case of uniform magnetization. This reduction is of second order in M/H_0, however, whereas the volume divergence and surface divergence at the sidefaces are of first order in this parameter.

Consider now the demagnetizing field along the center axis of the sample and compare its magnitude for the case of uniform magnetization to that for the case of the actual distribution of magnetization. The net magnetic field along the center axis assuming uniform magnetization is indicated as a broken line in Fig. 1(c). If we disregard the change in surface divergence at the endface (which is justified for reasonably large applied fields) the net field associated with the actual distribution of magnetization differs from that associated with uniform magnetization by the field arising from the volume divergence and the surface divergence at the sidefaces. Figures 1(a) and 1(b) show that this field is negative at the endface ($z=0$) but positive for large z. In both cases the contribution of the positive volume charge is larger (in magnitude) than the contribution of the negative surface charge, because the positive charge is closer to the observation point. The net field arising from the two charge clouds is (along the axis) directed away from the center of gravity of the two clouds. Thus the additional demagnetizing fields add to the demagnetizing field for uniform magnetization at $z=0$ but subtract from it for large enough z. This behavior has been confirmed by the detailed calculations presented in Sec. IIIB (compare Fig. 14). The solid line in Fig. 1(c) shows in a qualitative way how the net magnetic field varies along the center axis of the sample. It should be noticed that the actual demagnetizing field in the center of the endface is larger in magnitude than the demagnetizing field corresponding to uniform magnetization.

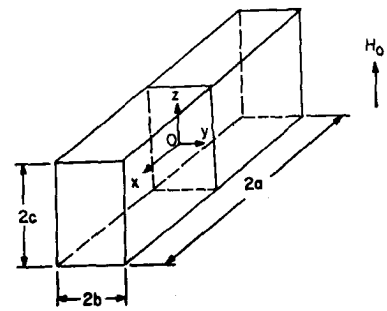

FIG. 2. Coordinate system as used in calculations pertaining to rectangular prisms (except semi-infinite prisms, compare Fig. 6). The origin of the coordinate system coincides with the center of the prism. The dc field H_0 is applied along the z direction.

By similar arguments, it can be shown that the z component of the demagnetizing field at the corner of the endface is smaller than that corresponding to uniform magnetization. This is demonstrated in Fig. 1(d).

In dealing with the ellipsoidal samples it is frequently convenient to express the demagnetizing field in terms of a tensorial demagnetization factor N_{ij} by means of the relation

$$H_i^{(\mathrm{dem})} = -4\pi \sum_j N_{ij} M_j = -4\pi M \sum_j N_{ij}\alpha_j, \quad (13)$$

where $H_i^{(\mathrm{dem})}$ is the i component of the demagnetizing field and $M_j = M\alpha_j$ the j component of the magnetization vector. Because Eq. (13) represents a linear relationship between two vector quantities, it follows immediately that N_{ij} transforms as a tensor. For nonellipsoidal samples, however, the relationship between

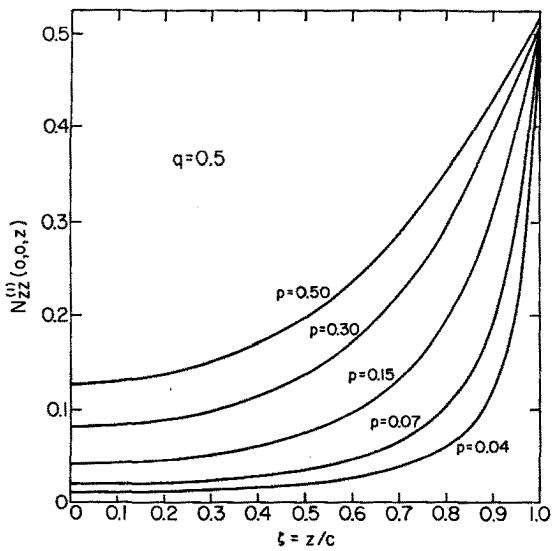

FIG. 3. The spatial variation of the first-order demagnetizing factor $N_{zz}^{(1)}$ along a coordinate axis of the prism ($x=y=0$) in terms of a reduced variable $\zeta\equiv z/c$ (z is the distance from the *center* of the prism) for various sample shapes ($q\equiv a/c=0.5$, $p\equiv b/c$). Note that $N_{zz}^{(1)}(-z)=N_{zz}^{(1)}(z)$.

demagnetizing field and magnetization is not, in general, linear by virtue of the higher-order correction terms in Eq. (8). For this reason the demagnetizing field cannot, in general, be expressed in terms of a tensorial demagnetizing factor (at least not in terms of a tensor of rank two). The first-order demagnetizing field, however, can always be represented in this way, even for nonellipsoidal samples. The demagnetizing factor is, of course, then a function of position.

$$H_i^{(1)}(\mathbf{r})=-4\pi M\sum_j N_{ij}^{(1)}(\mathbf{r})\alpha_j. \tag{14}$$

Here

$$\mathbf{H}^{(1)}(\mathbf{r})=M\nabla\psi_1(\mathbf{r}), \tag{15}$$

where ψ_1 is the first term of the expansion (8).

III. APPLICATION TO RECTANGULAR PRISMS

A. First-Order Theory

The demagnetizing field in uniformly magnetized, rectangular prisms has previously been considered by Rhodes and Rowlands.[6] These authors have evaluated the energy associated with certain pole distributions on the surface of rectangular prisms. In regard to the uniformly magnetized rectangular prisms their result is equivalent to a calculation of the spatial average of the first-order demagnetizing field. They do not give any results concerning the local demagnetizing field and its spatial variation.

The notation used in the following calculation is summarized in Fig. 2. The origin of the coordinate system coincides with the center of the prism and the axes are aligned with the principal axes of the prism. The lengths of the axes are $2a$, $2b$, and $2c$.

We express the first-order demagnetizing field in terms of a tensorial demagnetization factor $N_{ij}^{(1)}(\mathbf{r})$ as defined by Eq. (14). It is shown in Appendix A that the zz component of the demagnetization factor is given by

$$\begin{aligned}N_{zz}^{(1)}(\mathbf{r})=(1/4\pi)\{&\cot^{-1}f(x,y,z)+\cot^{-1}f(-x,y,z)\\&+\cot^{-1}f(x,-y,z)+\cot^{-1}f(x,y,-z)\\&+\cot^{-1}f(-x,-y,z)+\cot^{-1}f(x,-y,-z)\\&+\cot^{-1}f(-x,y,-z)\\&+\cot^{-1}f(-x,-y,-z)\},\end{aligned} \tag{16}$$

where

$$f(x,y,z)=\frac{[(a-x)^2+(b-y)^2+(c-z)^2]^{\frac{1}{2}}(c-z)}{(a-x)(b-y)}. \tag{17}$$

The principal value of the inverse cotangent should be taken (i.e., $0\leq\cot^{-1}f\leq\pi$). In Figs. 3–5 we plot the spatial variation of $N_{zz}^{(1)}(\mathbf{r})$ in various directions and locations in the sample for different sized samples.

The other two diagonal tensor components of the demagnetization factor (N_{xx} and N_{yy}) can be inferred from Eqs. (16) and (17) by interchanging x, y, and z and similarly a, b, and c [see Eq. (A10) of Appendix B]. The three diagonal tensor components obey the sum rule

$$N_{xx}^{(1)}(\mathbf{r})+N_{yy}^{(1)}(\mathbf{r})+N_{zz}^{(1)}(\mathbf{r})=1. \tag{18}$$

A general proof of this theorem has been given previously.[7] Rowlands[8] and Brown and Morrish[9] have earlier demonstrated a similar theorem for the average demagnetizing factor (the average being taken over

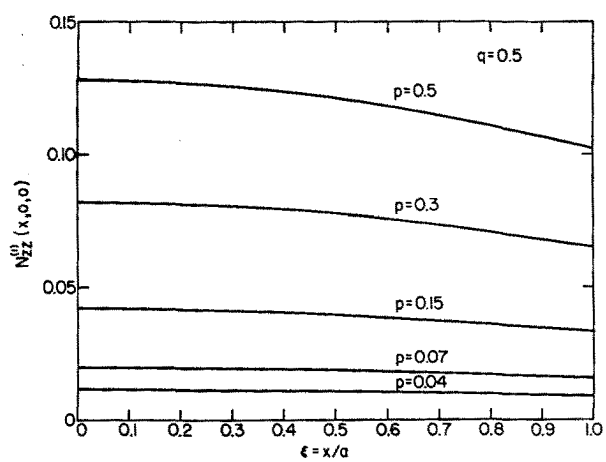

FIG. 4. The spatial variation of the first-order demagnetizing factor $N_{zz}^{(1)}$ along a coordinate axis of the prism ($y=z=0$) in terms of a reduced variable $\xi\equiv x/a$ (x is the distance from the center of the sample) for various sample sizes ($q\equiv a/c=0.5$, $p\equiv b/c$). Note that $N_{zz}^{(1)}(-x)=N_{zz}^{(1)}(x)$.

[6] P. Rhodes and G. Rowlands, Proc. Leeds Phil. Lit. Soc. Sci. Sec. **6**, 191 (1954).

[7] E. Schlömann, J. Appl. Phys. **33**, 2825 (1962).

[8] G. Rowlands, thesis, University of Leeds (1956).

[9] W. F. Brown, Jr., and A. H. Morrish, Phys. Rev. **105**, 1198 (1957).

the sample volume). We show in Appendix B that the analytic expressions derived for the rectangular prism actually satisfy the sum rule (18).

The off-diagonal tensor components of the demagnetization factor are also calculated in Appendix A. The xz component is given by

$$N_{xz}^{(1)}(\mathbf{r})=-\frac{1}{4\pi}\log\left\{\frac{G(\mathbf{r}|a,b,c)G(\mathbf{r}|-a,-b,c)G(\mathbf{r}|-a,b,-c)G(\mathbf{r}|a,-b,-c)}{G(\mathbf{r}|-a,b,c)G(\mathbf{r}|a,-b,c)G(\mathbf{r}|a,b,-c)G(\mathbf{r}|-a,-b,-c)}\right\}, \tag{19}$$

where

$$G(\mathbf{r}|a,b,c)=(b-y)+[(a-x)^2+(b-y)^2+(c-z)^2]^{\frac{1}{2}}. \tag{20}$$

The other off-diagonal tensor components of the demagnetization factor can be inferred from Eqs. (19) and (20) by suitable substitution. For instance, N_{yz} is obtained by interchanging x and y, and a and b, in Eq. (20).

In some applications the gradient of the demagnetizing field taken in the direction of the applied field is of particular importance. One finds readily from Eq. (16)

$$\partial N_{zz}^{(1)}(\mathbf{r})/\partial z=(1/4\pi)\{K(x,y,z)+K(-x,y,z)+K(x,-y,z)+K(-x,-y,z) -K(x,y,-z)-K(-x,y,-z)-K(x,-y,-z)-K(-x,-y,-z)\}, \tag{21}$$

where

$$K(x,y,z)=\frac{(a-x)(b-y)[(a-x)^2+(b-y)^2+2(c-z)^2]}{[(a-x)^2+(b-y)^2+(c-z)^2]^{\frac{1}{2}}[(a-x)^2+(c-z)^2][(b-y)^2+(c-z)^2]}. \tag{22}$$

The demagnetizing field near the endface $z=-c$ of the sample can be expanded in a power series in $z+c$. The lower-order derivatives of $N_{zz}^{(1)}$ taken at $z=-c$ are, for $x=y=0$ in the limit $c\gg a, b$, given by

$$\begin{aligned} &N_{zz}^{(1)}=\tfrac{1}{2}\\ &\partial N_{zz}^{(1)}/\partial z=-(a^2+b^2)^{\frac{1}{2}}/\pi ab\\ &\partial^2 N_{zz}^{(1)}/\partial z^2=0\\ &\partial^3 N_{zz}^{(1)}/\partial z^3=(2a^4+a^2b^2+2b^4)/\pi a^3b^3(a^2+b^2)^{\frac{1}{2}}. \end{aligned} \tag{23}$$

We conclude this section by a discussion of the special case in which the sample is much longer in the x and z directions than in the y direction (i.e., $a, c\gg b$). In this case the first-order demagnetizing field is much simpler than for a general rectangular prism. This fact makes it possible to evaluate explicitly the second-order demagnetizing field, as shown in Sec. IIIB.

Because a significant variation of the demagnetizing field occurs only near the endfaces, it is advantageous to describe the problem in a coordinate system, whose origin lies on the endface of the semi-infinite slab. Figure 6 shows the coordinate system used in the subsequent calculation.

The first-order demagnetizing factors for this situa-

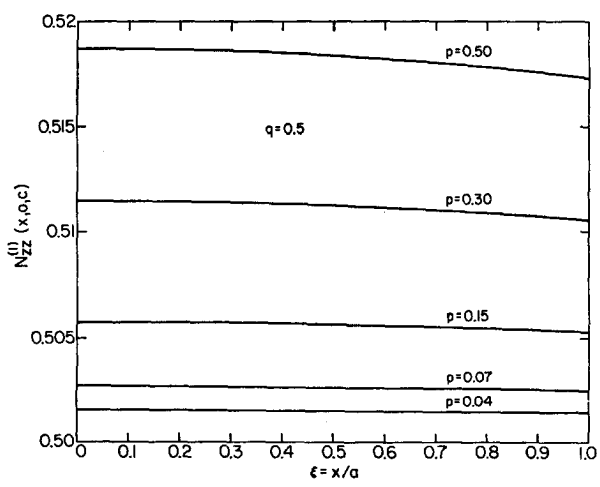

FIG. 5. The spatial variation of the first-order demagnetizing factor $N_{zz}^{(1)}$ along an axis on the edge of the prism ($y=0, z=c$) in terms of a reduced variable $\xi=x/a$ (x is the distance from the center of the sample) for various sample sizes ($q\equiv a/c=0.5$, $p\equiv b/c$). Note that $N_{zz}^{(1)}(-x)=N_{zz}^{(1)}(x)$.

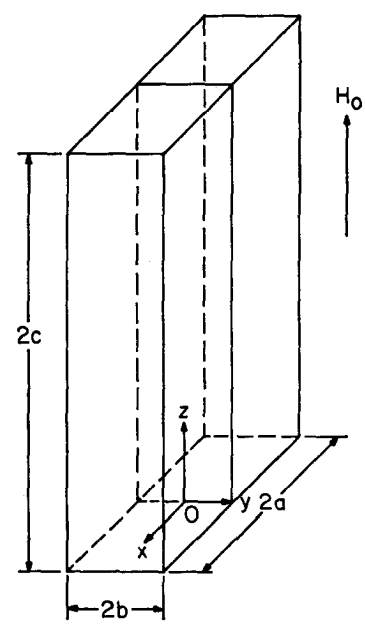

FIG. 6. Coordinate system used in calculations pertaining to the semi-infinite rectangular prism ($a, c\gg b$). The origin of coordinates coincides with the center of the endface of the prism perpendicular to the dc field H_0 (applied along the z direction). z now measures the distance from the endface.

tion are, according to Eqs. (16), (17), (19), and (20),

$$N_{zz}^{(1)}(\mathbf{r})=\frac{1}{2\pi}\left[\cot^{-1}\left(\frac{z}{b-y}\right)+\cot^{-1}\left(\frac{z}{b+y}\right)\right]$$
$$=\frac{1}{2\pi}\cot^{-1}\left(\frac{y^2+z^2-b^2}{2bz}\right) \tag{24}$$

$$N_{yz}^{(1)}(\mathbf{r})=\frac{1}{4\pi}\log\left[\frac{(b+y)^2+z^2}{(b-y)^2+z^2}\right]$$
$$=\frac{1}{2\pi}\coth^{-1}\left(\frac{y^2+z^2+b^2}{2by}\right), \tag{25}$$

and under the present conditions $N_{xx}^{(1)}(\mathbf{r})$ is identically zero.

Consider now the lines of constant $N_{zz}^{(1)}$ and constant $N_{yz}^{(1)}$ in the yz plane. If the sample is infinitely long in the x direction these sets of lines are mutually orthogonal regardless of the shape of the sample in the yz plane. This follows from the fact that the first-order magnetostatic potential ψ_1 satisfies Laplace's equation. In the present case of a semi-infinite slab the lines of constant $N_{zz}^{(1)}$ are circles whose centers lie on the z axis. They are described by the equation

$$y^2+[z-b\cot(2\pi N_{zz}^{(1)})]^2=b^2\csc^2(2\pi N_{zz}^{(1)}). \tag{26}$$

The lines of constant $N_{yz}^{(1)}$ are circles whose centers lie on the y axis. These lines are described by the equation

$$[y-b\coth(2\pi N_{yz}^{(1)})]^2+z^2=b^2\,\mathrm{csch}^2(2\pi N_{yz}^{(1)}). \tag{27}$$

Both sets of lines are indicated by the dashed lines in Fig. 7.

B. Second-Order Theory for Semi-Infinite Slabs

In the plane $x=0$ the second-order potential ψ_2 is, according to Eqs. (11), (14) and (25), given by

$$\psi_2(y,z)=-\int_{-\infty}^{+\infty}dx'\int_{-b}^{+b}dy'\int_0^{\infty}dz'\log\left[\frac{(b+y')^2+z'^2}{(b-y')^2+z'^2}\right]\frac{y'-y}{[x'^2+(y'-y)^2+(z'-z)^2]^{\frac{3}{2}}} \tag{28}$$

or, after integration over x',

$$\psi_2(y,z)=-2\int_{-b}^{+b}dy'\int_0^{\infty}dz'\log\left[\frac{(b+y')^2+z'^2}{(b-y')^2+z'^2}\right]\frac{y'-y}{(y'-y)^2+(z'-z)^2}. \tag{29}$$

We have here written $\psi_2(y,z)$ for $\psi_2(0,y,z)$. We define the second-order demagnetizing factor $N_{zz}^{(2)}$ by

$$N_{zz}^{(2)}(\mathbf{r})=-(1/4\pi)[\partial\psi_2(\mathbf{r})/\partial z]. \tag{30}$$

This demagnetizing factor describes the z component of the demagnetizing field for the case in which the sample is magnetized in the z direction.

For convenience we introduce normalized variables

$$\eta=y/b,\quad \zeta=z/b,\quad t=z'/b. \tag{31}$$

We show in Appendix C that the second-order demagnetizing factor can be expressed for $\eta=0$ as

$$N_{zz}^{(2)}(0,\zeta)=\frac{2}{\pi}\int_0^{\infty}dt\left\{\tfrac{1}{2}(t-\zeta)\left[\frac{1+\zeta^2-2\zeta t}{(1+\zeta^2)[1+(\zeta-2t)^2]}-\frac{1}{1+(\zeta-t)^2}\right]\log\left(\frac{4+t^2}{t^2}\right)\right.$$
$$\left.+\frac{2}{1+(\zeta-2t)^2}\tan^{-1}\left(\frac{1}{t-\zeta}\right)+\frac{2t(t-\zeta)}{(1+\zeta^2)[1+(\zeta-2t)^2]}\left[2\tan^{-1}\left(\frac{1}{t-\zeta}\right)-\tan^{-1}\frac{2}{t}\right]\right\}. \tag{32}$$

Note that as written, each of the three integrals appearing in Eq. (32) converges. In Fig. 8 we give the result of a numerical integration for $N_{zz}^{(2)}(0,\zeta)$. We have also plotted on the same figure the curve of $(\partial/\partial\zeta)N_{zz}^{(2)}(0,\zeta)$. A check on the accuracy of the integrations is the value of the derivative at $\zeta=0$. Here the derivative integrals may be evaluated exactly with the result $(\partial/\partial\zeta)N_{zz}^{(2)}(0,0)=-8/3$.

It is also shown in Appendix C that the second-order demagnetizing factor for $\zeta=0$ is

$$N_{zz}^{(2)}(\eta,0)=\frac{1}{\pi}\int_0^{\infty}dt\left\{-\tfrac{1}{2}\frac{t}{(1+\eta)^2+t^2}\log\left(\frac{4+t^2}{t^2}\right)+\frac{1}{(1+\eta)[(1+\eta)^2+4t^2]}\left[\tfrac{1}{2}t(1+\eta)\log\left\langle\frac{(4+t^2)}{t^2}\frac{(t^2+[1+\eta]^2)}{(t^2+[1-\eta]^2)}\right\rangle\right.\right.$$
$$\left.\left.+(1+\eta)^2\left\langle\tan^{-1}\left(\frac{1+\eta}{t}\right)+\tan^{-1}\left(\frac{1-\eta}{t}\right)\right\rangle+2t^2\left\langle\tan^{-1}\left(\frac{1+\eta}{t}\right)+\tan^{-1}\left(\frac{1-\eta}{t}\right)-\tan^{-1}\left(\frac{2}{t}\right)\right\rangle\right]\right\}+(\eta\to-\eta). \tag{33}$$

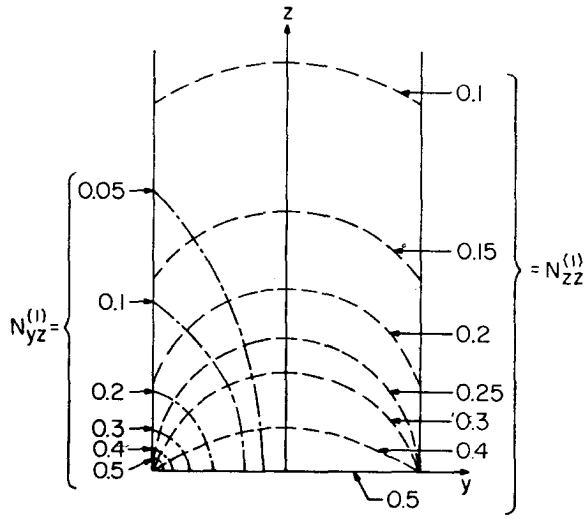

FIG. 7. Lines of constant $N_{zz}^{(1)}$ and constant $N_{yz}^{(1)}$ in the yz plane for a semi-infinite slab.

The terms not explicitly shown are to be derived from those given by changing η into $-\eta$.

In Fig. 9 we plot the result of a numerical integration for $N_{zz}^{(2)}(\eta,0)$. The vertical scale on the left side of the figure is to be used in the present discussion. The significance of the right-hand vertical scale and the horizontal line is discussed in Sec. V. In Eqs. (32) and (33) the principal value of the inverse tangent is to be taken (i.e., $-\pi/2 \leq \tan^{-1} f \leq \pi/2$).

IV. APPLICATION TO CIRCULAR CYLINDERS

A. First-Order Theory

We now consider a circular cylinder of diameter $2a$ and height L oriented as shown in Fig. 10. Equation

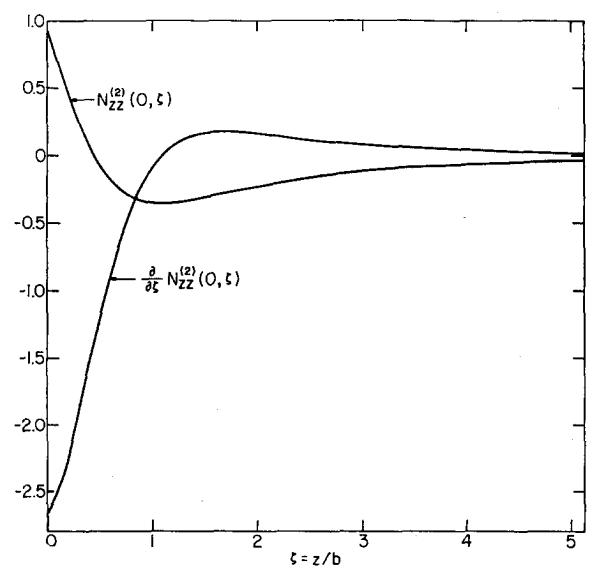

FIG. 8. The spatial variation of the second-order demagnetizing factor $N_{zz}^{(2)}$ along a coordinate axis of the semi-infinite prism ($x=y=0$) in terms of a reduced variable $\zeta=z/b$ (z is the distance from the *edge* of the prism). Also shown is the spatial variation of the gradient of the second-order demagnetizing factor in the same direction $(\partial/\partial\zeta)N_{zz}^{(2)}$ in reduced units.

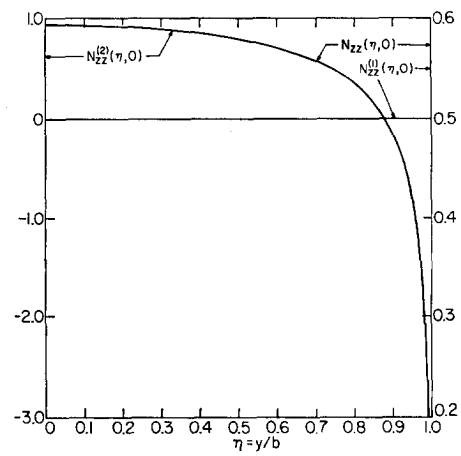

FIG. 9. The spatial variation of the first-order $N_{zz}^{(1)}$, second-order $N_{zz}^{(2)}$, and total demagnetizing factor N_{zz} in the endface ($x=z=0$) of a semi-infinite prism as a function of distance from the central axis (z) in terms of a reduced variable $\eta=y/b$. The vertical scale on the left side of the figure gives the values of $N_{zz}^{(2)}$ while the vertical scale on the right side of the figure gives the values of $N_{zz}^{(1)}$ and N_{zz}. A value of $\epsilon=\frac{1}{10}$ was used to compute N_{zz}. Note that $N_{zz}^{(2)}(y)=N_{zz}^{(2)}(-y)$.

(10) then gives for the present case

$$\psi_1(\mathbf{r}) = -\int_0^a r'dr' \int_0^{2\pi} d\theta' \times\{[r^2+r'^2+(L-z)^2-2rr'\cos(\theta-\theta')]^{-\frac{1}{2}} -[r^2+r'^2+z^2-2rr'\cos(\theta-\theta')]^{-\frac{1}{2}}\}. \quad (34)$$

Along the central axis of the cylinder ($r=0$, $0\leq z\leq L$) these integrals may be trivially evaluated with the result[10]:

$$\psi_1(0,z) = 2\pi a^2([z+(a^2+z^2)^{\frac{1}{2}}]^{-1} -\{(L-z)+[a^2+(L-z)^2]^{\frac{1}{2}}\}^{-1}), \quad (35)$$

where we have denoted $\psi_1(\mathbf{r})$ by $\psi_1(r,z)$. An alternative

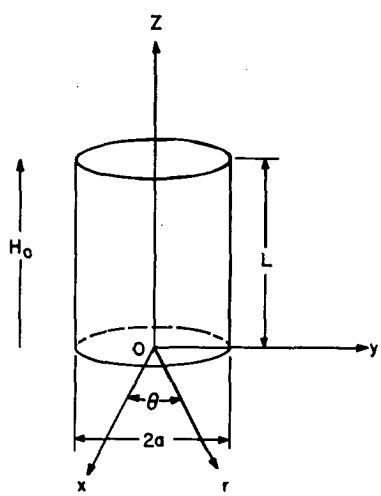

FIG. 10. Coordinate system used for calculations pertaining to the circular cylinder. The origin of coordinates coincides with the center of the circular endface of the cylinder which is oriented perpendicular to the applied dc field H_0 (applied along the z direction). z measures the distance from the endface.

[10] A. Sommerfeld, *Electrodynamics, Lectures on Theoretical Physics* (Academic Press Inc., New York, 1952), Vol. III, pp. 79–86.

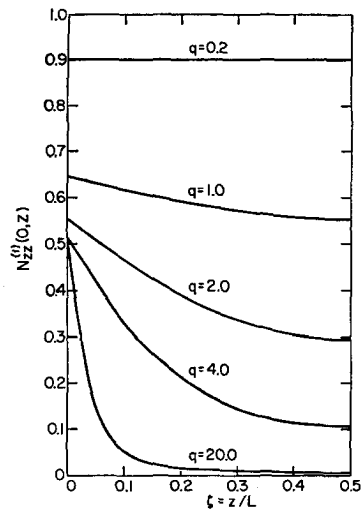

FIG. 11. The spatial variation of the first-order demagnetizing factor $N_{zz}^{(1)}$ along the central axis of the cylinder ($r=0$) in terms of a reduced variable $\zeta\equiv z/L$ for various sample shapes ($q\equiv L/a$). Note that $N_{zz}^{(1)}(z)=N_{zz}^{(1)}(L-z)$.

and simpler-appearing expression for $\psi_1(\mathbf{r})$ may be readily found. We may write

$$\psi_1(r,z)=\int_0^\infty J_0(tr)e^{-tz}\phi_1(t)dt + \int_0^\infty J_0(tr)e^{-t(L-z)}\phi_2(t)dt, \quad 0\leq z\leq L; 0\leq r\leq a. \tag{36}$$

$J_0(x)$ is the Bessel function of real argument of order zero. This expression satisfies the appropriate differential equation and boundary conditions. We determine the quantities $\phi_1(t)$ and $\phi_2(t)$ from the correspondence between Eqs. (35) and (36) with the result[11]

$$\phi_1(t)=-\phi_2(t)=2\pi aJ_1(ta)/t. \tag{37}$$

These integrals may be written in terms of the complete elliptic integrals of the first, second, and third kind.[12] The components of the demagnetizing field can now be readily obtained. From Eqs. (36) and (37), together with the definition (14), we find that the zz component of the demagnetization factor is given by

$$N_{zz}^{(1)}(r,z)=-(1/4\pi)(\partial/\partial z)\psi_1(r,z) =\tfrac{1}{2}a\int_0^\infty J_0(tr)J_1(ta)\{e^{-tz}+e^{-t(L-z)}\}dt, \tag{38}$$

from which it follows[12]

$$N_{zz}^{(1)}(r,z)=\{1-[zk_1K(k_1)/4\pi(ar)^{\frac{1}{2}}]-[\Lambda_0(\alpha_1,\beta_1)/4] -[(L-z)k_2K(k_2)/4\pi(ar)^{\frac{1}{2}}]-[\Lambda_0(\alpha_2,\beta_2)/4]\}, \tag{39}$$

where $K(k)$ is the complete elliptic integral of the first kind. $\Lambda_0(\alpha,\beta)$ is essentially the complete elliptic integral of the third kind introduced and tabulated by Heuman.[12]

$$\begin{cases} k_1^2=\dfrac{4ar}{z^2+(a+r)^2} \\ \sin\alpha_1=k_1 \\ \sin\beta_1=\dfrac{z}{[z^2+(a-r)^2]^{\frac{1}{2}}} \end{cases} \qquad \begin{cases} k_2^2=\dfrac{4ar}{(L-z)^2+(a+r)^2} \\ \sin\alpha_2=k_2 \\ \sin\beta_2=\dfrac{(L-z)}{[(L-z)^2+(a-r)^2]^{\frac{1}{2}}}, \end{cases} \tag{40}$$

In Figs. 11–13 we show the spatial variation of $N_{zz}^{(1)}(\mathbf{r})$ in various directions and locations in the sample, and for different sized samples. We note from Eq. (38), that in the limit $L\to\infty$, we have[13]

$$N_{zz}^{(1)}(r,0)=\tfrac{1}{2}a\int_0^\infty J_0(tr)J_1(ta)dt=\tfrac{1}{2}, \quad r<a. \tag{41}$$

The same result derives from the appropriate limit of Eqs. (39) and (40).

From Eqs. (36) and (37) we have

$$\frac{\partial\psi_1(r,z)}{\partial r}=-2\pi a\int_0^\infty J_1(tr)J_1(ta)\{e^{-tz}-e^{-t(L-z)}\}dt \tag{42}$$

from which it follows, together with definition (14), that[12] the rz component of the demagnetization factor is given by

$$N_{rz}^{(1)}(\mathbf{r})=-(1/4\pi)[\partial\psi_1(r,z)/\partial r] =(1/\pi)(a/r)^{\frac{1}{2}}\{(1/k_1)[(1-\tfrac{1}{2}k_1^2)K(k_1)-E(k_1)] -(1/k_2)[(1-\tfrac{1}{2}k_2^2)K(k_2)-E(k_2)]\}. \tag{43}$$

$E(k)$ is the complete elliptic integral of the second kind. k_1 and k_2 are given by Eq. (40). This quantity may be alternatively expressed in terms of the hypergeometric

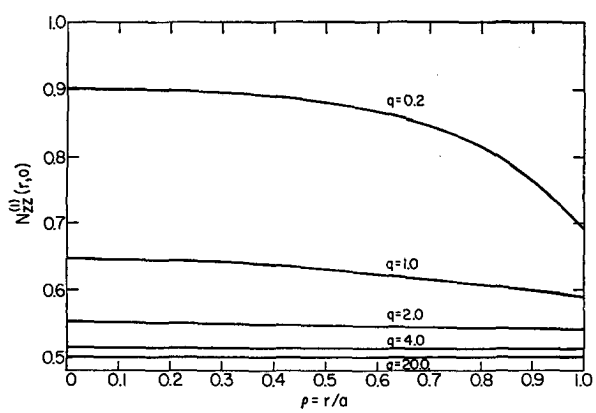

FIG. 12. The spatial variation of the first-order demagnetizing factor $N_{zz}^{(1)}$ in the endface of a circular cylinder ($z=0$) as a function of the distance from the central axis (z) in terms of a reduced variable $\rho=r/a$ for various sample shapes ($q=L/a$).

[11] A. Erdélyi, *Tables of Integral Transformations*, Bateman Manuscript Project (McGraw-Hill Book Company, Inc., New York, 1954), Vol. I, p. 182, No. 5.

[12] Y. L. Luke, *Integrals of Bessel Functions* (McGraw-Hill Book Company, Inc., New York, 1962), pp. 314–318.

[13] G. N. Watson, *Theory of Bessel Functions* (Cambridge University Press, Cambridge, 1952), 2nd ed., p. 406, No. 9.

function ${}_2F_1$. We have from Eq. (42)[14]

$$N_{rz}^{(1)}(\mathbf{r}) = -(1/4\pi)[\partial\psi_1(r,z)/\partial r] = \tfrac{1}{4}(a/r)^{\frac{1}{2}}\{(2R_1)^{-\frac{3}{2}}{}_2F_1(\tfrac{3}{4},\tfrac{5}{4};2;1/R_1^2) - (2R_2)^{-\frac{3}{2}}{}_2F_1(\tfrac{3}{4},\tfrac{5}{4};2;1/R_2^2)\}, \quad (44)$$

where

$$R_1 = (r^2+z^2+a^2)/2ra$$
$$R_2 = (r^2+(L-z)^2+a^2)/2ra. \quad (45)$$

We conclude this section by exhibiting an expression for the z component of the gradient of the zz component of the demagnetization factor. From Eq. (38) it follows that[12]

$$(\partial/\partial z)N_{zz}^{(1)}(r,z) = -(1/4\pi)(ra)^{-\frac{1}{2}}\left\{k_1K(k_1) + \frac{k_1^3(a^2-r^2-z^2)E(k_1)}{4ar(1-k_1^2)} - k_2K(k_2) - \frac{k_2^3(a^2-r^2-[L-z]^2)E(k_2)}{4ar(1-k_2^2)}\right\}. \quad (46)$$

k_1 and k_2 are given by Eq. (40). Either from Eq. (46) or the appropriate derivatives of Eq. (35), it follows that in the limit of $L\to\infty$

$$(\partial/\partial z)N_{zz}^{(1)}(0,0) = -(1/2a). \quad (47)$$

B. Second-Order Theory for Semi-Infinite Cylinders

In this section, we let the length of the cylinder L become infinite. Further, we restrict our attention to the point $r=z=0$. It then follows from Eqs. (11), (44), and (45) that

$$\psi_2(0,z) = -2\pi^2a^2\int_0^a r'^3dr'\int_0^\infty dz'\frac{{}_2F_1(\frac{3}{4},\frac{5}{4};2;[4r'^2a^2/(r'^2+z'^2+a^2)^2])}{[r'^2+(z-z')^2]^{\frac{3}{2}}[r'^2+z'^2+a^2]^{\frac{3}{2}}} \quad (48)$$

so that

$$\frac{\partial\psi_2(0,0)}{\partial z} = -6\pi^2\int_0^1\rho^3d\rho\int_0^\infty\zeta d\zeta\frac{{}_2F_1(\frac{3}{4},\frac{5}{4};2;[4\rho^2/(\rho^2+\zeta^2+1)^2])}{[\rho^2+\zeta^2+1]^{\frac{3}{2}}[\rho^2+\zeta^2]^{\frac{3}{2}}} \quad (49)$$

and

$$\frac{\partial^2\psi_2(0,0)}{\partial z^2} = \frac{6\pi^2}{a}\lim_{\epsilon\to0}\int_0^1\rho^3d\rho\int_0^\infty d\zeta\frac{{}_2F_1(\frac{3}{4},\frac{5}{4};2;[4\rho^2/(\rho^2+\zeta^2+1)^2])}{[\rho^2+\zeta^2+1]^{\frac{3}{2}}}\times\frac{\partial}{\partial\zeta}\left(\frac{\zeta-\epsilon}{[\rho^2+(\zeta-\epsilon)^2]^{\frac{3}{2}}}\right). \quad (50)$$

We have introduced the dimensionless variables $\rho=r'/a$, $\zeta=z'/a$, and $\epsilon=z/a$ in Eqs. (49) and (50) so that the double integrals that appear in these expressions are simply numerical coefficients. The evaluation of these numerical factors is discussed in detail in Appendixes D and E, respectively. The results may thus be written as

$$N_{zz}^{(2)}(0,0) = \tfrac{3}{8}\pi\alpha \quad (51)$$

$$(\partial/\partial z)N_{zz}^{(2)}(0,0) = -\tfrac{3}{2}\pi\beta/a, \quad (52)$$

where α and β are numbers of order unity and have the approximate values

$$\alpha\approx1.0 \quad (53)$$

$$\beta\approx0.87. \quad (54)$$

The second-order demagnetizing factor $N_{zz}^{(2)}$ is defined by Eq. (30).

V. DISCUSSION

The total demagnetizing factor is, according to Eqs. (8), (14), and (30), given by

$$N_{zz}(\mathbf{r}) = N_{zz}^{(1)}(\mathbf{r}) + \epsilon N_{zz}^{(2)}(\mathbf{r}) + \cdots. \quad (55)$$

A comparison between the results obtained for semi-infinite slabs and semi-infinite cylinders is instructive. At the center of the endface of a semi-infinite slab the total demagnetizing factor and its gradient are, according to Eq. (23) and Fig. 8,

$$N_{zz} = \tfrac{1}{2}[1+1.9\epsilon+\cdots]$$
$$\partial N_{zz}/\partial z = -(1/\pi b)[1+8.4\epsilon+\cdots]. \quad (56)$$

At the center of the endface of a semi-infinite cylinder,

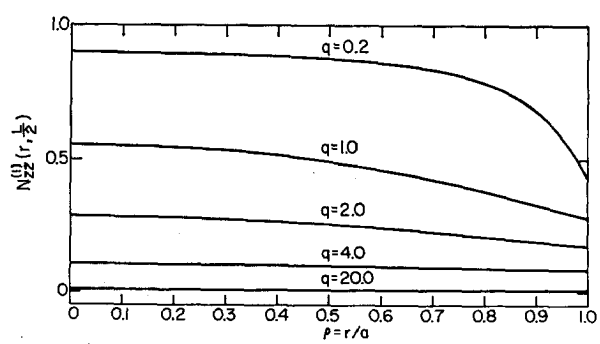

FIG. 13. The spatial variation of the first-order demagnetizing factor $N_{zz}^{(1)}$ in a plane parallel to the endfaces and equidistant from both ($z=L/2$) as a function of the distance from the central axis (z) in terms of a reduced variable $\rho=r/a$ for various sample shapes ($q=L/a$).

[14] A. Erdélyi, *Tables of Integral Transformations*, Bateman Manuscript Project (McGraw-Hill Book Company, Inc., New York, 1954), Vol. I, p. 183, No. 14 and p. 370.

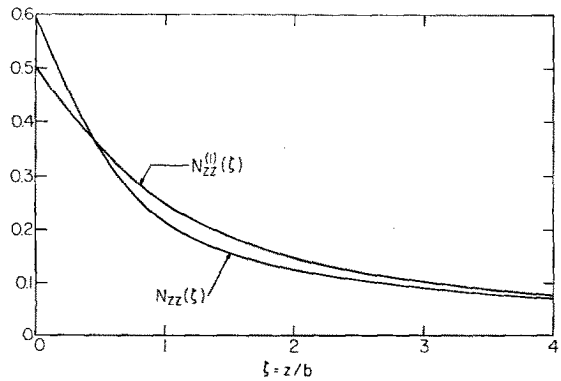

FIG. 14. The spatial variation of the first-order $N_{zz}^{(1)}$, and total demagnetizing factor N_{zz}, along a coordinate axis of the semi-infinite prism ($x=y=0$) in terms of a reduced variable $\zeta=z/b$ (z is the distance from the *edge* of the prism) for a value of $\epsilon=\frac{1}{10}$.

on the other hand, the same quantities are, according to Eqs. (41), (47), and (51)–(54),

$$N_{zz}=\tfrac{1}{2}[1+2.4\epsilon+\cdots]$$
$$\partial N_{zz}/\partial z=-(1/2a)[1+8.2\epsilon+\cdots]. \quad (57)$$

Comparison of Eqs. (56) and (57) shows that the fractional change in the total demagnetizing field or its gradient due to the second-order correction is approximately the same in the two sample shapes. It appears very likely, therefore, that the second-order demagnetizing field in cylinders will have approximately the same spatial dependence as that calculated for the case of semi-infinite slabs (Fig. 8). It should also be noted that the second-order correction affects the field gradient much more strongly than the field itself.

Consider now the spatial variation of the total demagnetizing factor for semi-infinite slabs. In Fig. 14 the total demagnetizing factor along the central axis is plotted as a function of the distance from the endface for a typical value of $\epsilon(\epsilon=\frac{1}{10})$. Also shown for comparison is the result of the first-order theory ($\epsilon=0$). It is obvious from this figure that the second-order correction is most important near the endface of the sample.

The variation of the demagnetizing factor across the endface has been briefly discussed in connection with Fig. 9. The scale on the right side of this figure refers to the total demagnetizing factor (again assuming $\epsilon=\frac{1}{10}$). In the first approximation ($\epsilon=0$) the demagnetizing factor is constant across the endface.

Kohane, Schlömann, and Joseph[5] have recently reported the experimental observation of magnetoelastic resonances in the nonuniform magnetic field near the endface of rectangular slabs. From these experiments the field gradient along the center axis can be inferred. The observations are in good agreement with the calculations presented in the present paper.

ACKNOWLEDGMENTS

The authors would like to thank Miss W. Doherty and Mrs. J. Newell for their aid with the numerical work and Dr. J. A. Mullen for several helpful discussions.

APPENDIX A—DEMAGNETIZING FIELD IN RECTANGULAR PRISMS IN FIRST APPROXIMATION

For the configuration described by Fig. 2, the first-order potential $\psi_1(\mathbf{r})$ is, according to Eq. (10),

$$\psi_1(\mathbf{r})=-\int_{-a}^{+a}dx'\int_{-b}^{+b}dy' \times\{[(x'-x)^2+(y'-y)^2+(c-z)^2]^{-\frac{1}{2}} -[(x'-x)^2+(y'-y)^2+(c+z)^2]^{-\frac{1}{2}}\}. \quad (A1)$$

Here we have used the identity

$$-(\partial/\partial z')(1/|\mathbf{r}'-\mathbf{r}|)=(z'-z)/|\mathbf{r}'-\mathbf{r}|^3. \quad (A2)$$

The xz component of the demagnetization factor is, according to our definitions,

$$N_{xz}^{(1)}(\mathbf{r})=-(1/4\pi)[\partial\psi_1(\mathbf{r})/\partial x]. \quad (A3)$$

Since differentiation with respect to x is, apart from the sign, equivalent to differentiation with respect to x', we obtain, from Eqs. (A1) and (A3),

$$N_{xz}^{(1)}(\mathbf{r})=-\frac{1}{4\pi}\int_{-b}^{+b}dy'\{[(a-x)^2+(y'-y)^2+(c-z)^2]^{-\frac{1}{2}}-[(a+x)^2+(y'-y)^2+(c-z)^2]^{-\frac{1}{2}} -[(a-x)^2+(y'-y)^2+(c+z)^2]^{-\frac{1}{2}}+[(a+x)^2+(y'-y)^2+(c+z)^2]^{-\frac{1}{2}}\}. \quad (A4)$$

Equation (19) now follows by straightforward integration.

The zz component of the demagnetization factor is

$$N_{zz}^{(1)}(\mathbf{r})=-(1/4\pi)[\partial\psi_1(\mathbf{r})/\partial z]. \quad (A5)$$

According to Eq. (A1), $N_{zz}^{(1)}(\mathbf{r})$ is

$$N_{zz}^{(1)}(\mathbf{r})=\frac{1}{4\pi}\int_{-a}^{+a}dx'\int_{-b}^{+b}dy'\left\{\frac{c-z}{[(x'-x)^2+(y'-y)^2+(c-z)^2]^{\frac{3}{2}}}+\frac{c+z}{[(x'-x)^2+(y'-y)^2+(c+z)^2]^{\frac{3}{2}}}\right\}, \quad (A6)$$

or, after integration over y',

$$N_{zz}^{(1)}(\mathbf{r})=\frac{1}{4\pi}\int_{-a}^{+a}dx'\left\{\frac{c-z}{(x'-x)^2+(c-z)^2}\left(\frac{b-y}{[(x'-x)^2+(b-y)^2+(c-z)^2]^{\frac{1}{2}}}+\frac{b+y}{[(x'-x)^2+(b+y)^2+(c-z)^2]^{\frac{1}{2}}}\right)\right.$$
$$\left.+\frac{c+z}{(x'-x)^2+(c+z)^2}\left(\frac{b-y}{[(x'-x)^2+(b-y)^2+(c+z)^2]^{\frac{1}{2}}}+\frac{b+y}{[(x'-x)^2+(b+y)^2+(c+z)^2]^{\frac{1}{2}}}\right)\right\}. \quad (A7)$$

The remaining integrations over x' can be carried out by first breaking up the range of integration into two parts: $x'=-a$ through x, and $x'=x$ through a, and then by noting that

$$\frac{d}{dx'}\cot^{-1}\frac{[(x'-x)^2+b^2+c^2]^{\frac{1}{2}}c}{(x'-x)b}$$
$$=\frac{bc}{[(x'-x)^2+c^2][(x'-x)^2+b^2+c^2]^{\frac{1}{2}}}. \quad (A8)$$

The inverse cotangent is restricted to its principal value. Equation (16) then follows immediately.

APPENDIX B—SUM RULE FOR THE DEMAGNETIZATION FACTOR OF RECTANGULAR PRISMS

According to Eq. (16), the trace of the demagnetization factor is

$$\sum_i N_{ii}^{(1)}(\mathbf{r})=(1/4\pi)\{[\cot^{-1}f(\mathbf{r})+\cot^{-1}g(\mathbf{r})+\cot^{-1}h(\mathbf{r})]+\cdots\}. \quad (A9)$$

Here $f(\mathbf{r})$ is given by Eq. (17) and

$$g(\mathbf{r})=[(a-x)^2+(b-y)^2+(c-z)^2]^{\frac{1}{2}}(b-y)/(a-x)(c-z)$$
$$h(\mathbf{r})=[(a-x)^2+(b-y)^2+(c-z)^2]^{\frac{1}{2}}(a-x)/(b-y)(c-z). \quad (A10)$$

The terms not explicitly shown in Eq. (A9) can be derived from those shown by replacing x by $-x$, etc. in the manner of Eq. (16). The sum rule now follows by noting that

$$\cot^{-1}f+\cot^{-1}g+\cot^{-1}h=\cot^{-1}\left[\frac{fgh-f-g-h}{fg+fh+hg-1}\right], \quad (A11)$$

and that, according to Eqs. (17) and (A10),

$$fgh-f-g-h=0. \quad (A12)$$

Each bracket in Eq. (A9) equals $\pi/2$.

APPENDIX C—EVALUATION OF INTEGRALS INVOLVED IN $N_{zz}^{(2)}(y,z)$ (SEMI-INFINITE SLAB)

By partial integration and using

$$(y'-y)/[(y'-y)^2+(z'-z)^2]=\tfrac{1}{2}(\partial/\partial y')\log[(y'-y)^2+(z'-z)^2], \quad (A13)$$

Eq. (29) can be written as

$$\psi_2(y,z)=-\int_0^\infty dz'F(z'|y,z), \quad (A14)$$

where

$$F(z'|y,z)=\log[(4b^2+z'^2)/z'^2]\log\{[(b+y)^2+(z'-z)^2][(b-y)^2+(z'-z)^2]\}$$
$$-2\int_{-b}^{+b}dy'\log[(y'-y)^2+(z'-z)^2]\left[\frac{b+y'}{(b+y')^2+z'^2}+\frac{b-y'}{(b-y')^2+z'^2}\right]. \quad (A15)$$

According to Eqs. (30) and (A14), the second-order demagnetizing factor is given as an integral over $\partial F/\partial z$. From (A15)

$$\frac{\partial F(z'|y,z)}{\partial z}=-2(z'-z)\left[\frac{1}{(b+y)^2+(z'-z)^2}+\frac{1}{(b-y)^2+(z'-z)^2}\right]\log\left(\frac{4b^2+z'^2}{z'^2}\right)$$
$$+4\int_{-b}^{+b}dy'\frac{z'-z}{(y'-y)^2+(z'-z)^2}\left[\frac{b+y'}{(b+y')^2+z'^2}+\frac{b-y'}{(b-y')^2+z'^2}\right]. \quad (A16)$$

The integration over y' can be carried out by using the identity

$$\int dt\frac{\alpha t}{[(t-t_0)^2+\alpha^2](t^2+\beta^2)}=[(t_0^2+\alpha^2-\beta^2)^2+4t_0^2\beta^2]^{-1}$$
$$\times(\tfrac{1}{2}\alpha(t_0^2+\alpha^2-\beta^2)\log\{(t^2+\beta^2)/[(t-t_0)^2+\alpha^2]\}+t_0(t_0^2+\alpha^2+\beta^2)\tan^{-1}[(t-t_0)/\alpha]-2t_0\alpha\beta\tan^{-1}(t/\beta)). \quad (A17)$$

This can readily be verified by differentiation.

The two terms inside the bracket of the integrand in Eq. (A16) give rise to two contributions to $\partial F/\partial z$, each of which is of the form of Eq. (A17). The second integral can in fact be derived from the first by simply changing the signs of y and y'. With the substitutions

$$t=b+y',\ t_0=b+y,\ \alpha=z'-z,\ \beta=z',$$

the first integral in Eq. (A16) becomes identical with the integral of Eq. (A17). We therefore obtain

$$\frac{\partial F(z'|y,z)}{\partial z}=-\frac{2(z'-z)}{(b+y)^2+(z'-z)^2}\log\left(\frac{4b^2+z'^2}{z'^2}\right)+(4/\{[(b+y)^2+(z'-z)^2-z'^2]^2+4(b+y)^2z'^2\})$$
$$\times\left\{\tfrac{1}{2}(z'-z)[(b+y)^2+(z'-z)^2-z'^2]\log\left(\frac{[4b^2+z'^2]}{z'^2}\frac{[(b+y)^2+(z'-z)^2]}{[(b-y)^2+(z'-z)^2]}\right)\right.$$
$$+(b+y)[(b+y)^2+(z'-z)^2+z'^2]\left[\tan^{-1}\frac{b-y}{z'-z}+\tan^{-1}\frac{b+y}{z'-z}\right]$$
$$\left.-2(b+y)(z'-z)z'\tan^{-1}(2b/z')\right\}+(y\to -y). \quad \text{(A18)}$$

The terms not explicitly written down are to be derived from those given by changing y into $-y$. The principal values of the inverse tangent must be taken. The function $\partial F/\partial t$ is discontinuous at $z'=z$, where $\tan^{-1}[b/(z'-z)]$ jumps from $-\pi/2$ to $+\pi/2$. The mathematical reason for this discontinuity is the fact that the factor $\alpha/[(t-t_0)^2+\alpha^2]$ in Eq. (A17) approaches a different limit for $\alpha\to 0^+$ than for $\alpha\to 0^-$. It is well known that for $\alpha\to 0$

$$\alpha/[(t-t_0)^2+\alpha^2]\to(\alpha/|\alpha|)\pi\delta(t-t_0).$$

Expressed in terms of the reduced variables defined by Eq. (31), the second-order demagnetizing factor is, according to Eqs. (30), (A14), and (A18),

$$N_{zz}^{(2)}(\eta,\zeta)=\frac{1}{\pi}\int_0^\infty dl\left\{-\tfrac{1}{2}\frac{(l-\zeta)}{(1+\eta)^2+(l-\zeta)^2}\log\left(\frac{4+l^2}{l^2}\right)+\{[(1+\eta)^2+\zeta^2][(1+\eta)^2+(\zeta-2l)^2]\}^{-1}\right.$$
$$\times\left[\tfrac{1}{2}(l-\zeta)[(1+\eta)^2+\zeta^2-2\zeta l]\log\left\{\frac{(4+l^2)}{l^2}\frac{[(1+\eta)^2+(l-\zeta)^2]}{[(1-\eta)^2+(l-\zeta)^2]}\right\}+(1+\eta)[(1+\eta)^2+\zeta^2]\right.$$
$$\left.\left.\times\left(\tan^{-1}\frac{1+\eta}{l-\zeta}+\tan^{-1}\frac{1-\eta}{l-\zeta}\right)+2(1+\eta)l(l-\zeta)\left(\tan^{-1}\frac{1+\eta}{l-\zeta}+\tan^{-1}\frac{1-\eta}{l-\zeta}-\tan^{-1}\frac{2}{l}\right)\right]\right\}+(\eta\to-\eta). \quad \text{(A19)}$$

Equations (32) and (33) are now obtained by taking the appropriate special case ($\eta=0$ and $\zeta=0$, respectively).

APPENDIX D—EVALUATION OF INTEGRALS INVOLVED IN $N_{zz}^{(2)}(0,0)$ (SEMI-INFINITE CYLINDER)

From Eqs. (30), (49), and (51), we have

$$\alpha=\int_0^1 udu\int_0^\infty dv\frac{{}_2F_1(\frac{3}{4},\frac{5}{4};2;4u/(u+v+1)^2)}{(u+v+1)^{\frac{3}{2}}(u+v)^{\frac{1}{2}}}, \quad \text{(A20)}$$

where we have made the substitutions $\rho^2=u$, $\zeta^2=v$. Making use of the series representation of the hypergeometric function[15] then gives

$$\alpha=\sum_{n=0}^\infty A_n f_n, \quad \text{(A21)}$$

where

$$A_n=[(\tfrac{3}{4})_n(\tfrac{5}{4})_n/(2)_n n!]4^n, \quad \text{(A22)}$$

and

$$f_n=\int_0^1 duu^{n+1}g_n(u), \quad \text{(A23)}$$

with

$$g_n(u)=\int_0^\infty dv(u+v)^{-\frac{1}{2}}(u+v+1)^{-(\frac{3}{2}+2n)}. \quad \text{(A24)}$$

The quantities $(\sigma)_n$ are given by

$$(\sigma)_n=\sigma(\sigma+1)(\sigma+2)\cdots(\sigma+n-1)$$
$$(\sigma)_0=1. \quad \text{(A25)}$$

The substitution $v+(1+u)=z^{-1}$ (u considered constant)

[15] G. N. Watson, *Theory of Bessel Functions* (Cambridge University Press, Cambridge, 1952), 2nd ed., p. 100.

reduces $g_n(u)$ to the form

$$g_n(u)=\int_0^{(1+u)^{-1}} dz z^{2(n+1)}(1-z)^{-\frac{1}{2}} \qquad \text{(A26)}$$

which may be directly integrated with the result

$$g_n(u)=2\sum_{\nu=0}^{2n+2}\frac{(-1)^\nu\binom{2n+2}{\nu}}{4n-2\nu+1}\left[1-\left(\frac{u}{1+u}\right)^{2n-\nu+\frac{1}{2}}\right]. \qquad \text{(A27)}$$

Substituting this back into Eq. (A23) then gives

$$\tfrac{1}{2}f_n=\sum_{\nu=0}^{2n+2}\frac{(-1)^\nu\binom{2n+2}{\nu}}{4n-2\nu+1}\times\left\{\frac{1}{n+2}-\int_0^1 du\frac{u^{5n-2\nu+2}}{[u(1+u)]^{2n-\nu+\frac{1}{2}}}\right\}. \qquad \text{(A28)}$$

The integral in Eq. (A28) may be readily performed with the result

$$\begin{aligned}\tfrac{1}{2}f_n=&\sum_{\nu=0}^{2n+2}\frac{(-1)^\nu\binom{2n+2}{\nu}}{(4n-2\nu+1)(n+2)}-\left[\sum_{\nu=0}^{2n-1}\frac{(-1)^\nu\binom{2n+2}{\nu}}{(4n-2\nu+1)(n+2)!}\right.\\
&\times\left\{\sqrt{2}\sum_{\lambda=0}^{2n-\nu-1}\frac{(-1)^\lambda(n+2+\lambda)!2^{2\lambda-2n+\nu+1}}{(4n-2\nu-1;-2;\lambda+1)}\right.\\
&+\frac{(-1)^{2n-\nu}(3n-\nu+2)!2^{2n-\nu}}{(1;2;2n-\nu)}\left\langle\sqrt{2}\sum_{\lambda=1}^{3n-\nu+2}\frac{(-1)^{\lambda+1}(6n-2\nu+3;-2;\lambda-1)}{(3n-\nu+2;-1;\lambda)2^{\lambda-1}}\right.\\
&\left.\left.\left.+\frac{(-1)^{3n-\nu+2}(1;2;3n-\nu+2)}{(3n-\nu+2)!2^{3n-\nu+2}}\log(3+2\sqrt{2})\right\rangle\right\}\\
&+(n+1)(2n+1)\left\{\sqrt{2}\sum_{\lambda=1}^{n+2}\frac{(-1)^{\lambda+1}(2n+3;-2;\lambda-1)}{(n+2;-1;\lambda)2^{\lambda-1}}+\frac{(-1)^n(1;2;n+2)}{(n+2)!2^{n+2}}\log(3+2\sqrt{2})\right\}\\
&+(2n+\tfrac{5}{3})\left\{2\sqrt{2}\sum_{\lambda=1}^{n}\frac{(-1)^{\lambda-1}(2n+1;-2;\lambda-1)}{(n+2;-1;\lambda)2^{\lambda-1}}+\frac{(-1)^n(3;2;n)}{(3;1;n)2^n}\langle\tfrac{3}{4}\sqrt{2}-\tfrac{1}{8}\log(3+2\sqrt{2})\rangle\right\}\\
&-\tfrac{1}{3}\left\{2\sqrt{2}\sum_{\lambda=1}^{n-1}\frac{(2n-1;-2;\lambda-1)(-1)^{\lambda-1}}{(n+1;-1;\lambda)2^{\lambda-1}}+\frac{(-1)^{n-1}(3;2;n-1)}{(3;1;n-1)2^{n-1}}\langle\tfrac{3}{4}\sqrt{2}-\tfrac{1}{8}\log(3+2\sqrt{2})\rangle\right.\\
&\left.\left.+\delta_{n0}\langle\sqrt{2}+\tfrac{1}{2}\log(3+2\sqrt{2})\rangle\right\}\right]. \qquad \text{(A29)}\end{aligned}$$

This expression for f_n is valid for all $n\geq 0$. However, a word of clarification as to its interpretation for $n=0$ and $n=1$ is necessary. For these two cases, those summations in which the upper summation limit is less than the lower limit are to be discarded. Further, the term which for $n=0$ involves $(3;2;-1)$ is also to be discarded. δ_{n0} is the Kronecker delta and is different from zero only for $n=0$. We have

$$\begin{aligned}&(m;d;\nu)=m(m+d)(m+2d)\cdots(m+[\nu-1]d)\\
&(m;d;0)=1 \qquad \text{(A30)}\\
&(m;-d;\nu)=d^\nu\Gamma([m/d]+1)/\Gamma([m/d]-\nu+1).\end{aligned}$$

Explicit evaluation of the first few of the quantities f_n gives

$$\begin{aligned}&f_0=\tfrac{4}{3}(2-\sqrt{2})=0.78105\\
&f_1=(1/45)(256-179\sqrt{2})=0.06346 \qquad \text{(A31)}\\
&f_2=(1/1260)(10240-7233\sqrt{2})=0.00872.\end{aligned}$$

We note that in addition to the small numerical factor in front of the parentheses of Eq. (A31), it is the close cancellation of the factors inside the parentheses which is essential for the rapid convergence of the series. Substituting these results in Eq. (A21) together with Eq. (A22) then gives

$$\begin{aligned}\alpha&=0.78105+0.11899+0.04292+\cdots\\
&=0.943+\cdots \qquad \text{(A32)}\end{aligned}$$

from which we obtain the result of Eq. (53).

APPENDIX E—EVALUATION OF INTEGRALS INVOLVED IN $(\partial/\partial z)N_{zz}^{(2)}(0,0)$ (SEMI-INFINITE CYLINDER)

From Eqs. (30), (50), and (52), we obtain

$$\begin{aligned}2\beta=&-\int_0^1 udu\int_0^\infty dvv^{\frac{1}{2}}(u+v)^{-\frac{1}{2}}\\
&\times\frac{\partial}{\partial v}\left[\frac{{}_2F_1(\frac{3}{4},\frac{5}{4};2;4u/(1+u+v)^2)}{(1+u+v)^{\frac{1}{2}}}\right]\\
&+\lim_{\epsilon\to 0}\epsilon\int_0^1 duu(u+\epsilon^2)^{-\frac{1}{2}}{}_2F_1(\tfrac{3}{4},\tfrac{5}{4};2;4u/(1+u)^2)\\
&\times(1+u)^{-\frac{1}{2}}\equiv 2\beta_1+2\beta_2, \qquad \text{(33A)}\end{aligned}$$

where we have performed an integration by parts and made the substitutions $u=\rho^2$, $v=\zeta^2$ and set $\epsilon=0$ in the first integral since the resultant integral is perfectly regular. Consider the first integral of Eq. (A33). Making use of the series representation of the hypergeometric function, gives, upon performing the indicated differentiation, the result

$$\tfrac{4}{3}\beta_1=\sum_{n=0}^{\infty}A_n(1+\tfrac{4}{3}n)h_n, \tag{A34}$$

where A_n is given by Eq. (A22) and

$$h_n=\int_0^1 duu^{n+1}k_n(u) \tag{A35}$$

with

$$k_n(u)=\int_0^\infty dvv^{\frac{1}{2}}(u+v)^{-\frac{5}{2}}(1+u+v)^{-(2n+\frac{5}{2})}. \tag{A36}$$

The substitution $v+(1+u)=(1-w)^{-1}$ (u considered constant) reduces $k_n(u)$ to the form

$$k_n(u)=(1+u)^{\frac{1}{2}}\int_{\alpha_2}^{\alpha_1}dw\frac{w^{-2}(\alpha_1-w)^{2n+3}(w-\alpha_2)}{[a_0(w-\alpha_1)(w-\alpha_2)(w-\alpha_3)]^{\frac{1}{2}}} \tag{A37}$$

with

$$\begin{aligned}&a_0=-1\\&\alpha_1=1\\&\alpha_2=u/1+u\\&\alpha_3=0\qquad(\alpha_1>\alpha_2\geq\alpha_3).\end{aligned} \tag{A38}$$

Use of the binomial theorem to expand the polynomial $(1-w)^{2n+3}$ reduces the integrals of Eq. (A37) to known forms[16] with the result[17]

$$k_n(u)=(1+u)^{\frac{1}{2}}\sum_{\lambda=0}^{2n+3}(-1)^\lambda\binom{2n+3}{\lambda}\times\{-J_{2n-\lambda+2}(\alpha_1)+\alpha_2J_{2n-\lambda+1}(\alpha_1)\} \tag{A39}$$

and where

$$J_{\pm n}(w)=\int\frac{w^{\pm n}dw}{[a_0(w-\alpha_1)(w-\alpha_2)(w-\alpha_3)]^{\frac{1}{2}}}. \tag{A40}$$

The quantities $J_{\pm n}(\alpha_1)$ satisfy the following recursion formulae[16]:

$$\begin{aligned}J_n(\alpha_1)=&\left(\frac{2n-2}{2n-1}\right)\left(\frac{1+2u}{1+u}\right)J_{n-1}(\alpha_1)\\&-\left(\frac{2n-3}{2n-1}\right)\left(\frac{u}{1+u}\right)J_{n-2}(\alpha_1),\\J_{-n}(\alpha_1)=&\left(\frac{2n-2}{2n-1}\right)\left(\frac{1+2u}{u}\right)J_{-n+1}(\alpha_1)\\&-\left(\frac{2n-3}{2n-1}\right)\left(\frac{u+1}{u}\right)J_{-n+2}(\alpha_1).\end{aligned} \tag{A41}$$

[16] W. Gröbner and N. Hofreiter, *Integraltafel, Erster Teil, Unbestimmte Integrale* (Springer-Verlag, Wein und Innsbruck, 1957), pp. 75–81.

[17] Terms of the form $J_m(\alpha_2)$ have been neglected since it can be shown that they all vanish.

It is evident from these recursion formulae that all of the $J_{\pm n}(\alpha_1)$ can be finally reduced to linear combinations of the quantities $J_{\pm1}(\alpha_1)$ and $J_0(\alpha_1)$ which can be written in terms of known functions. We have that[16]

$$\begin{aligned}J_1(\alpha_1)&=2E(k),\\J_0(\alpha_1)&=2K(k),\\J_{-1}(\alpha_1)&=(2/1-k^2)E(k),\end{aligned} \tag{A42}$$

where $K(k)$ and $E(k)$ are the complete elliptic integrals of the first and second kinds, respectively, with

$$k^2=(1+u)^{-1}. \tag{A43}$$

Substitution of the results of Eqs. (A37)–(A43) in Eq. (A35) then yields for h_n

$$h_n=\int_{\frac{1}{2}}^1 dx\frac{(1-x)^n}{x^{\frac{1}{2}}x^{n+3}}\times\{\alpha_n(x)E(x^{\frac{1}{2}})+\beta_n(x)[(1-x)K(x^{\frac{1}{2}})]\}, \tag{A44}$$

where we have made the additional substitution $k^2=x$. $\alpha_n(x)$ and $\beta_n(x)$ are polynomials in x, of degree $2n+2$ and $2n+1$, respectively, which can be directly obtained. We restrict our further discussion to the first few coefficients h_n. One thus finds that

$$\begin{aligned}&\tfrac{3}{2}h_0=A_0-8B_0\\&A_0=\int_{\frac{1}{2}}^1 dx\frac{E}{x^3x^{\frac{1}{2}}}\{16-16x+x^2\}\\&B_0=\int_{\frac{1}{2}}^1 dx\frac{[(1-x)K]}{x^3x^{\frac{1}{2}}}\{2-x\}\end{aligned} \tag{A45}$$

$$\begin{aligned}&\tfrac{3}{2}h_1=(1/35)(A_1-2B_1)\\&A_1=\int_{\frac{1}{2}}^1 dxE\left\{\frac{(1-x)}{x^4x^{\frac{1}{2}}}\right\}\{1280-1408x+126x^2+29x^3+8x^4\}\\&B_1=\int_{\frac{1}{2}}^1 dx[(1-x)K]\left\{\frac{(1-x)}{x^4x^{\frac{1}{2}}}\right\}\times\{640-384x-9x^2-2x^3\}\end{aligned} \tag{A46}$$

$$\begin{aligned}&\tfrac{3}{2}h_2=(1/1155)(A_2-4B_2)\\&A_2=\int_{\frac{1}{2}}^1 dxE\left\{\frac{(1-x)^2}{x^5x^{\frac{1}{2}}}\right\}\{71680-81920x+8000x^2+2112x^3+811x^4+344x^5+128x^6\}\\&B_2=\int_{\frac{1}{2}}^1 dx[(1-x)K]\left\{\frac{(1-x)^2}{x^5x^{\frac{1}{2}}}\right\}\{17920-11520x-400x^2-152x^3-57x^4-16x^5\}.\end{aligned} \tag{A47}$$

We have there written E and K for $E(x^{\frac{1}{2}})$ and $K(x^{\frac{1}{2}})$, respectively.

The integrals $A_{0,1,2}$ and $B_{0,1,2}$ must be numerically performed with the results

$$\begin{aligned} A_0&=14.331\\ A_1&=705.69\\ A_2&=28968.60, \end{aligned} \tag{A48}$$

and

$$\begin{aligned} B_0&=1.765\\ B_1&=352.50\\ B_2&=7241.46, \end{aligned} \tag{A49}$$

so that one finds

$$\begin{aligned} \tfrac{3}{2}h_0&=0.211\\ \tfrac{3}{2}h_1&=(1/35)(0.69)\\ \tfrac{3}{2}h_2&=(1/1155)(2.76). \end{aligned} \tag{A50}$$

Again we note that the close cancellation between A and λB is essential for the convergence.

Using these results in Eq. (A34) together with Eq. (A22) then gives

$$\begin{aligned} 2\beta_1&=0.211+0.086+0.043+\cdots\\ &=0.340+\cdots. \end{aligned} \tag{A51}$$

Consider now the second integral of Eq. (A33). For $\epsilon\rightarrow 0$ the main contribution to the integral is from the vicinity of $u=0$. We then have

$$2\beta_2=\lim_{\epsilon\rightarrow 0}\epsilon\int_0^1 du\, u(u+\epsilon^2)^{-\frac{1}{2}}\{1+0(u)\}, \tag{A52}$$

where we have expanded the last two terms in the integrand in a power series in u. These integrals may now be directly performed with the result

$$2\beta_2=\tfrac{4}{3}, \tag{A53}$$

from which, together with Eq. (A51), we obtain the result of Eq. (54).

JOURNAL OF APPLIED PHYSICS VOLUME 36, NUMBER 5 MAY 1965

Effect of Temperature on the Mechanical Properties of Solid Pressure-Transmitting Media. II. Pyrophyllite

C. O. Hulse and R. B. Graf
Research Laboratories, United Aircraft Corporation, East Hartford, Connecticut
(Received 5 October 1964)

The high-temperature compressive strength of block pyrophyllite is not significantly less than the room-temperature strength at temperatures below 1200° and it is noticeably greater at 600° and 1100°C. The major increase in strength occurs above 1050°C and is associated with the decomposition of the pyrophyllite to mullite and silica phases. This increase in ultimate strength is time dependent and may amount to as much as five times the room-temperature strength. Because pyrophyllite is also used as a thermal insulator in high-temperature high-pressure applications, a shell of this stronger material will be present around samples heated for long times above 1050°C. This may adversely affect its efficiency as a solid pressure-transmitting medium. Pyrophyllite is superior to talc for similar high-temperature applications because it can be dehydrated prior to use without increasing its strength, and it develops its high-temperature strength more slowly.

INTRODUCTION

MASSIVE pyrophyllite is the most widely used solid pressure-transmitting medium. When finely ground it behaves as a clay mineral and is often used to give forming strength to ceramic ware and as a source of alumina and silica to fired pieces. The massive varieties of both pyrophyllite and talc have the desirable characteristics of being easily machined while at the same time being good electrical and thermal insulators. These particular properties are responsible for their use as solid pressure-transmitting media in the various devices now in use. Pyrophyllite is preferred over talc where sufficient internal friction is necessary to form a gasket and seal the high-pressure chamber, as in the multi-anvil and belt pressure devices.

Pyrophyllite has been shown to exhibit a considerable variation in pressure-transmitting qualities.[1] It has also been reported that pyrophyllite may contain up to about 25 wt % impurities, the most important of which are the similar layer materials, diapore and halloysite.[2] Further complications in its use in high-pressure devices at high temperatures are introduced by dehydration, which occurs at temperatures between 400° and 700°C.[3] This is accompanied by some expansion due to sepa-

[1] J. Tydings and A. Giardini, ASME Publ. 63-WA-307 (1962).
[2] E. Bradbury *et al.*, "Effects of Ultrahigh Pressures on the Formation and Properties of Organic, Semiorganic, and Inorganic Materials," Tech. Doc. Rept. No. ASD-TDR-62-73, Directorate of Materials and Processes, Wright Patterson AFB (1962).
[3] C. Parmelee and L. Barrett, J. Am. Ceram. Soc. **21**, 388 (1938).